Models for symmetric cold rolling of an aluminum sheet

János György Bátorfi[a,b]*, Gyula Pál[a,b], Purnima Chakravarty[a,b], Jurij Sidor[a]

[a] *ELTE, Faculty of Informatics, Savaria Institute of Technology*
[b] *ELTE, Faculty of Science, Doctoral School of Physics*

ABSTRACT

In the current work, the behavior of Al alloys during cold rolling is studied with the help of numerical approaches such as Finite Element (FEM) and Flow-Line (FLM) Models. The applicable simplifications for each method have been summarized in this contribution. For simulating the process of rolling, a material model was employed, which is based on the measured values obtained from the tensile test. The results of the conducted rolling experiments were compared with the numerical simulations performed by employing the experimental material models. The analysis of simulated and experimental data allowed us to evaluate the friction coefficient. A relationship has been established between the minimum friction coefficient necessary for rolling and the estimated one and this result is in a good agreement with the counterpart reported in literature sources. The established method was used for the evaluation of the characteristic components of the strain, namely the normal, shear, and equivalent components. The comparative study between recorded measurements and simulations indicates that both the FEM and FLM models can be successfully applied to simulate the symmetric cold rolling process of aluminum with sufficient accuracy.

Keywords: *cold rolling, aluminum, finite element model, flow-line model*

1. Introduction

The coefficient of friction enforces a strong effect on the deformation paths during the process of rolling. This technological parameter expresses the rate of shear and normal stresses in the contacts of the sheet and the rolls, as it is expressed among others by Avitzur [2]. There are many models for describing the deformation rate as a function of various technological and physical parameters such as temperature, slip velocity in the contact, normal pressure, the shear strength of the sheets material, or the roughness of the surface [3, 4], however, in this study, a simple approximation is used with a constant value.

The presented work aims to compare various calculation techniques for estimating the strain values at different points of the sheet during the cold rolling process. The results of the analytical approximation employed were compared to the experimental counterparts. Various physical parameters were determined by these calculations, for example, the friction coefficient, which describes the frictional properties. The experimentally observed deformation flow was likewise compared to the results of FEM simulations.

*Corresponding author: János György Bátorfi, bj@inf.elte.hu
https://doi.org/10.37775/EIS.2022.2.1

2. Tensile and rolling samples

The FEM simulations required a material model, the parameters of which were determined from the strain-stress curve, obtained by the tensile test. Prior to tensile testing and rolling experiments, the samples were heat-treated at 550 °C for 3 min for reducing the effect of previous thermo-mechanical treatments. The samples were prepared from a sheet of Al-1050 with an initial thickness of 2 mm. Gauge length and initial cross section of the tensile samples are 50 mm and 18.44 mm^2 respectively. The strain and stress values are calculated by Eq. (1) and (2), as described by Santaoja [5, 6].

$$\varepsilon = \ln\left(1 + \frac{\Delta l}{l_0}\right), \tag{1}$$

$$\sigma = \frac{F}{A_0}\left(1 + \frac{\Delta l}{l_0}\right). \tag{2}$$

The strain-stress diagram is shown in Fig. 1. The tensile test data are fitted by the Ramberg-Osgood material model by using Eq. (3) [7, 8]:

$$\varepsilon = \frac{\sigma}{E} + \left(\frac{\sigma}{K}\right)^{1/c} \tag{3}$$

The parameters of the material model are presented in Table 1. The correlation factor for the measured and fitted values is 0.9996. The rolling was performed with geometrical dimensions described in Table 2.

Table 1. Parameters for the Ramberg-Osgood material model

Parameter	Value
E [GPa]	69.9
K [MPa]	144.6
c [-]	0.37

Table 2. Parameters of cold rolling

Parameter	Value
Radius of the roll, R [mm]	75
Initial thickness of the sheet, h_i, [mm]	2
Sheet thickness following rolling, h_f, [mm]	1.4
Angular velocity of the rolls, ω, [rad/s]	1.1023

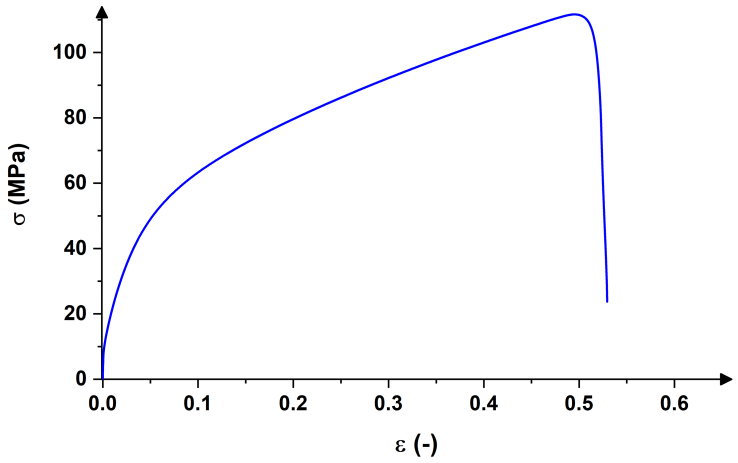

Figure 1. Strain-stress values for tensile test

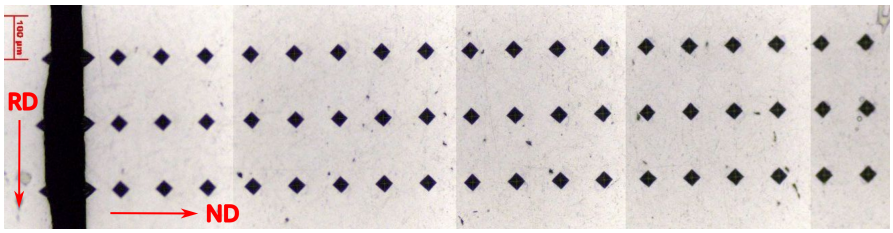

Figure 2. The prepared surface of the sheet prior to cold rolling

3. Rolling

In most general case, rolling can be defined as a widely used manufacturing process employed for reducing the thickness of materials. The rolling experiment is performed by pressing the sheet material between 2 rotating rolls. Based on the velocity of the bottom and top rolls, the rolling process can be defined as symmetric and asymmetric. On the other hand, based on temperature maintained during the deformation, symmetric and asymmetric rolling can be categorized as cold and hot rolling [9]. In this study, only the cold symmetrically rolled material has been studied. The geometrical model of the roll gap, showing the half-thickness of a rolled sheet is presented in Fig. 3. This simplified, half-geometry is used in the numerical models employed.

After rolling, the initially straight lines made of indents became distorted, and the displacements of the sheet layers are shown in Fig. 4. To further proceed with the study, the plane perpendicular to the transverse direction (TD plane) was grinded and polished, and afterward a pattern, consisting of numerous points, was created by microhardness indents as it is shown in Fig. 2.

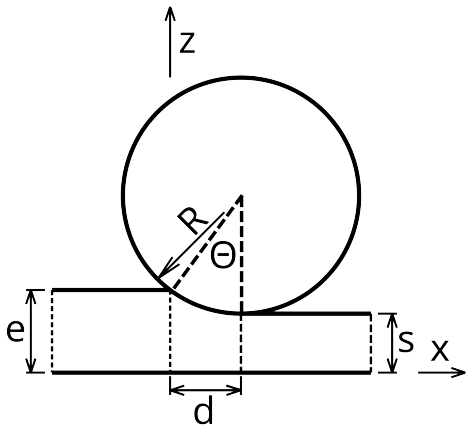

Figure 3. Simplified geometry used for FEM and FLM

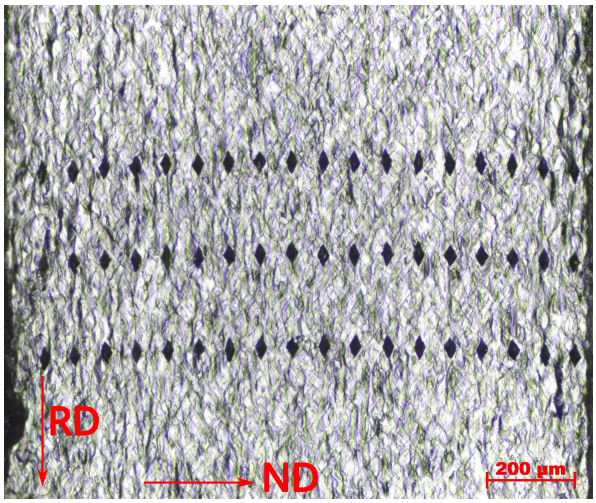

Figure 4. Distortion of initially straight lines caused by cold rolling

The displacement of a particular layer can be determined by the method developed by Boldetti [10], Roumina [11], and Ma [12]. The mentioned methodology allows us to calculate the strain values as it is described by Eq. (4-7) [12, 13]:

$$\varepsilon = \frac{h_i - h_f}{h_i}, \tag{4}$$

$$\gamma = \frac{dz}{dx}, \tag{5}$$

$$\varepsilon_S = \frac{2(1-\varepsilon)^2}{\varepsilon(2-\varepsilon)}\gamma \cdot \ln\frac{1}{1-\varepsilon}, \tag{6}$$

$$\varepsilon_{vM} = \sqrt{\frac{4}{3}\left(\ln\left(\frac{1}{1-\varepsilon}\right)\right)^2 + \frac{\varepsilon_S^2}{3}}, \tag{7}$$

where ε is a thickness reduction, z is a coordinate along the thickness of the sheet, x is a displacement of the sheet in the rolling direction, γ is a derivative of displacement of the sheet in the rolling direction, ε_S is the shear deformation, and ε_{vM} is a von Mises strain.

An important parameter of the rolling process is the friction coefficient μ, which is the result of a complex mechanism, effected by various physical parameters, as is summarised by Szűcs [3, 14] and Sidor [15]. The most important parameters allowing estimation of μ are the temperature, the pressure that acts on the surface, and the slip velocity between the sheet and the rolls [3]. According to a commonly used approximation, these dependencies can be neglected, and one can estimate a representative value of μ for the entire process, i.e. a constant μ is assumed for a given roll gap geometry. According to the model of Avitzur [16], a minimum value of friction coefficient can be determined by Eq. (8):

$$\mu_{min} = \frac{1}{2}\sqrt{\frac{h}{R}}\frac{\ln\left(\frac{h_i}{h_f}\right) + \frac{1}{4}\sqrt{\frac{h_i - h_f}{R}}}{\tan^{-1}\left(\frac{h_i}{h_f} - 1\right)}. \tag{8}$$

The μ_{min} calculated by using the parameters presented in Table 2 is 0.049. Alternative models dealing with the friction are described in [3, 14, 16–22]. The studies can be extended with further parameters such as microstructural properties as described by Sidor [23].

4. Finite Element Model

Finite element modeling is a commonly used method to describe the deformation conditions of the manufacturing process [24–28]. In this study, the commercially available DEFORM 2D software [29] was used, which is designed for modeling the plastic deformation. For the simulation, the previously described Ramberg-Osgood model was used. The further parameters are set as described in Table 2, with the extension, that the friction coefficient was changed between the μ_{min} and $\mu = 0.25$.

The optimum value of the friction coefficient was determined by comparing the experimentally observed and simulated deformation patterns. The geometry of the roll gap is visible in Fig. 5. The

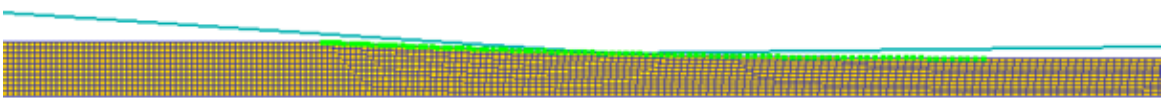

Figure 5. Rolling gap geometry used in the FEM simulation

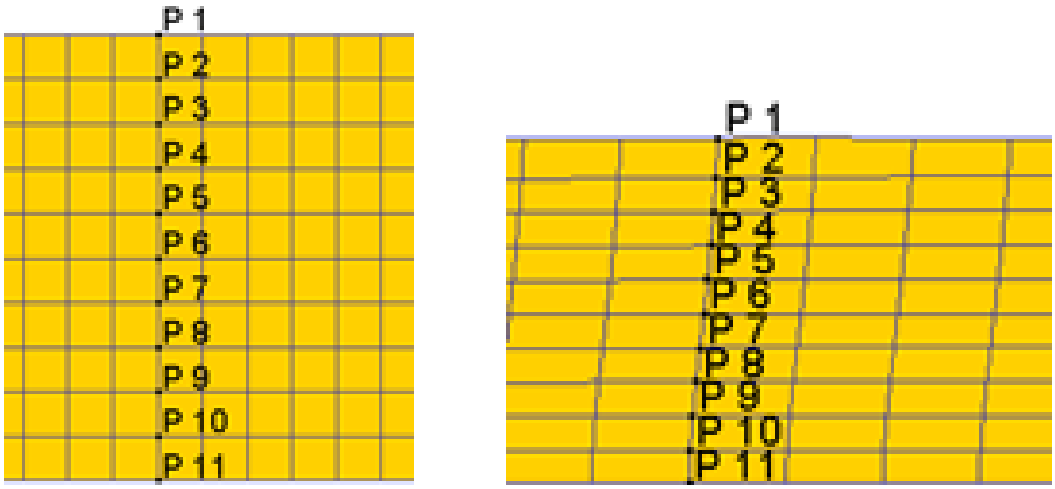

(a) (b)

Figure 6. a) Mesh prior to rolling, b) Mesh distortion after 30% rolling reduction

sheet was subdivided into 10 layers, while each layer contains identical square shaped elements. The meshed sheets before and after the rolling are presented in Figs. 6(a) and 6(b).

The deformation pattern extracted from the deformed sheet and the simulated counterparts with different constant friction coefficients are shown in Fig. 7. The wide-dashed line is the average displacement calculated from the 3 different measured line, the narrow-dashed line represents the tolerance limits calculated from the measured points, by adding and subtracting the standard deviations. It is important to mention, that the dx and z coordinates are equal to 0 on the symmetry plane of the rolled sheet. The estimated friction coefficient, based on a comparison of distorted lines, is approximately 0.068.

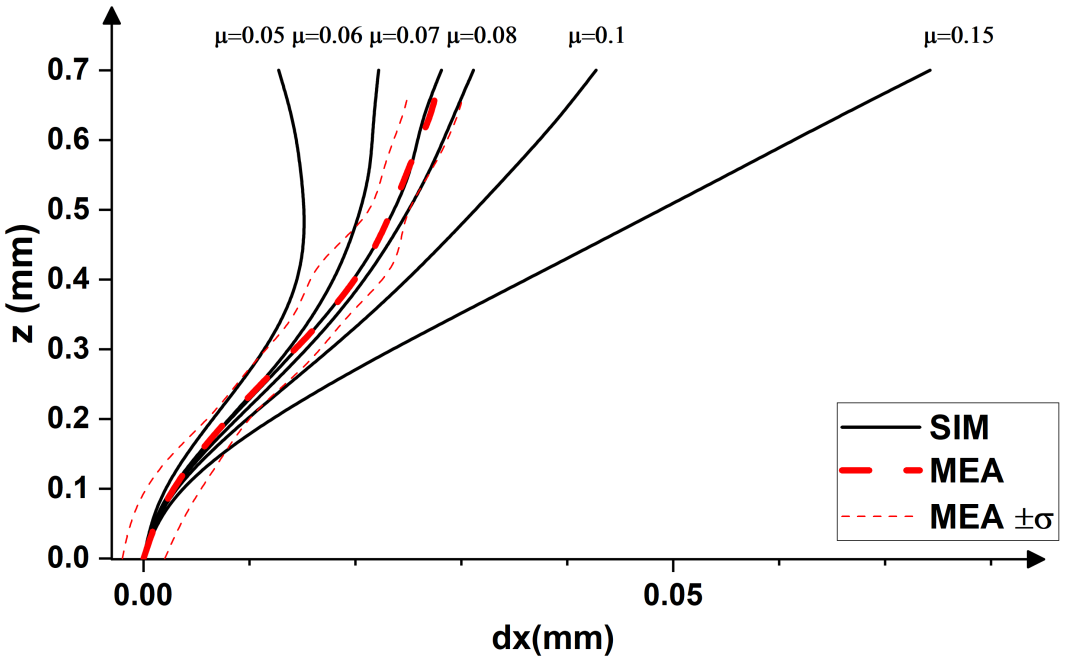

Figure 7. Deformation patterns of measured (MEA) and simulated displacements for 30% thickness reduction

5. Flow-Line Model (FLM)

There are different simplified numerical models, which can be used for a well-specified manufacturing process. The most commonly used types are based on simplified hydrodynamical models, for example, the Flow-Line Model (FLM) [30]. This model is based on the description of the virtual flowlines described by means of analytical functions. The model used in this study consist of a function expressed in the form of Eq. (9) by Beausir [30] and Decroos [31].

$$\Phi(x,z) = \frac{z_s}{\alpha} = z\left[1+\left(\alpha+\frac{(1-\alpha)(x-d)^2}{d^2}\right)^{-n}\right]^{1/n}, \tag{9}$$

where x, z coordinates on the sheet as defined in Fig. 3, z_s relative coordinate on the rolled sheet's thickness, α and n are later explained parameters used for describing the flowlines' deformation characteristics, the definition of these parameters are different for various models. For further calculations, it is important to define the following parameters:

$$\alpha = \frac{s}{e}, \tag{10}$$

$$\cos(\theta) = \frac{R+s-e}{R}, \tag{11}$$

$$d = R\sin(\theta), \tag{12}$$

where s half of the thickness after rolling, e half of the thickness before rolling, α is a parameter used for calculating the thickness's relative change, θ is the press angle, d is the projected length of pressed arc. By using these definitions, the velocity components for the directions can be defined by Eq. (13) and (14) as defined by Beausir [30].

$$v_x(x,z) = \lambda(x,z)\frac{\partial\,\Phi(x,z)}{\partial z}, \tag{13}$$

$$v_z(x,z) = -\lambda(x,z)\frac{\partial\,\Phi(x,z)}{\partial x}. \tag{14}$$

The $\lambda(x,z)$ function is defined by a velocity boundary condition in the exit points of the rolling gap, with Eq. (15) [30].

$$\lambda(x,z) = \frac{v_x(x=d,z)}{(\alpha^{-n}+1)^{1/n}}. \tag{15}$$

The velocity profile can be calculated by Eq. (16) [30].

$$v_x(x=d,z) = A\cdot z_s^2 + B\cdot z_s + C, \tag{16}$$

where A, B, and C parameters can be calculated by Eq. (17)-(23) [30].

$$A = v_0^t + v_0^b - 2\frac{v_0+v_n}{2s^2}, \tag{17}$$

$$B = \frac{v_0^t - v_0^b}{s2}, \tag{18}$$

$$C = v_0 + v_n, \tag{19}$$

$$v_0^t = \omega^t R, \tag{20}$$

$$v_0^b = \omega^b R, \tag{21}$$

$$v_0 = \frac{\omega^t+\omega^b}{2}R, \tag{22}$$

$$v_n = -pv_0, \tag{23}$$

where p parameter for describing the frictional conditions, w^t and w^b are the angular velocities for top and bottom rolls. By knowing the components of velocity, the velocity gradients can be expressed in general form with Eq. (24) by applying the theory of Beausir [30]:

$$L_{ij} = \frac{\partial v_i}{\partial j}. \tag{24}$$

The values of the displacement components were determined by Eq. (25) [24]:

$$D_{ij} = \int_0^L \frac{L_{ij}}{v_x} dx. \tag{25}$$

The strain tensor components can be calculated by Eq. (26).

$$\varepsilon_{ij} = \varepsilon_{ji} = \frac{D_{ij} + D_{ji}}{2}. \tag{26}$$

The fitted value for the parameter p is 0.0025.

6. Modified version of Flow-Line Model (mFLM)

In [15, 31] a partially modified version of the FLM model is described. The main difference compared to the previous version of FLM is that the flow line's definition and the definition of v_x velocity is different. The updated version is given by Eq. (27) and (28), this modified version was developed by Decroos [31]. Other numerical models are founded for example in [32–40].

$$\Phi(x,z) = \frac{z}{e}\left[1 + \left(\frac{s}{e} + \left(1 - \frac{s}{e}\right)\left(\frac{d-x}{d}\right)^{2.1}\right)^{-m}\right]^{1/m}, \tag{27}$$

$$v_x(x,z) = f_1(x) \cdot (1 - z_s)^n + f_2(x) \cdot z_s^n. \tag{28}$$

The $f_1(x)$ and $f_2(x)$ functions can be calculated from the boundary condition, by applying the Eq. (29) and (30) of the Decroos' theory [31].

$$\frac{1}{n+1} f_1(x) + \frac{1}{n+1} f_2(x) = v_{in} \cdot \left[1 + \left(\frac{s}{e} + \left(1 - \frac{s}{e}\right)\left(\frac{d-x}{d}\right)^{2.1}\right)^{-m}\right]^{1/m}, \tag{29}$$

$$f_2 - f_1 = \alpha \cdot \left\{ e \cdot v_{in} \cdot \left[1 + \left(\frac{s}{e} + \left(1 - \frac{s}{e}\right)\left(\frac{d-x}{d}\right)^{2.1}\right)^{-m}\right]^{1/m} - f_{1,ref} \right\}, \tag{30}$$

where, v_{in} is the velocity of the sheet before rolling, this value can be approximated by the angular velocity of rolls, m is an arbitrary parameter, in our study the, the applied value is 50. The $f_{1,ref}$ function can be defined by Eq. (31) [31].

$$f_{1,ref} = \left[1 - e^{-a\left(\frac{x}{d}\right)^b}\right]\left(\frac{e}{s} v_{in} - v_{in}\right) + v_{in}. \tag{31}$$

The parameter b in the Eq. (29)-(31) is an arbitrary number, in this study, the value of 3 was chosen according to reference [31]. This value was determined by comparing various simulation methods, by Decroos [31]. The parameter a is parameter based on the relative position of the neutral point, the

Table 3. Friction coefficients defined for various computational techniques

Method	Value
FEM	$\mu = 0.068$
FLM	$p = 0.0025$
mFLM	$\mu = 0.070$
Theory, Eq. (8)	$\mu = 1.4\mu_{\min} = 0.0685$

calculation method is described in [31]. Determination of α and n was done by the model of Sidor [15], which employs Eq. (32)-(34) for the estimation of both model parameters.

$$\Psi = \mu^{1.833} \cdot \left(\frac{h_i}{R}\right)^{0.789} \cdot \left(\frac{R}{h_i - h_f}\right)^{0.2293} \cdot \left(\frac{R}{h_f}\right)^{0.2983}, \tag{32}$$

$$\alpha = 21.332\Psi - 225\Psi^2 - 184.1\Psi^3 + 12420\Psi^4 + 0.4833\left(\frac{h_i - h_f}{2L_d}\right), \tag{33}$$

$$n = 19.369\mu^{0.09882}\left(\frac{h_i}{R}\right)^{0.00512} + 9.463\mu^{-0.1869}\left(\frac{L_d}{L_{dN}}\right)^{0.06414} - \tag{34}$$
$$- 18.606\mu^{-0.1045}\left(\frac{h_i + h_f}{R}\right)^{-0.00586} - 9.086\mu^{0.2441}\left(\frac{L_d}{h_i + h_f}\right)^{-0.162} + 0.03201,$$

where, L_d is the projected length of the pressed arc, L_{dN} is the position of the neutral point on the pressed arc, α and n are intermediate parameters used for the FLM model, these parameters have a different meaning, than in previous model. Substituting the values of roll gap geometry into Eq. (32)-(34) yields to the $\mu = 0.07$.

7. Comparison

The determined values of μ for each method are presented in Table 3. The estimated friction coefficients by the FEM and the mFLM are comparable to the μ_{min} (see Eq. (8)). It should be noted here that it is difficult to validate the accuracy of the FLM model since the model parameter p is not correlated directly with the μ. These obtained friction coefficients can be compared to the result

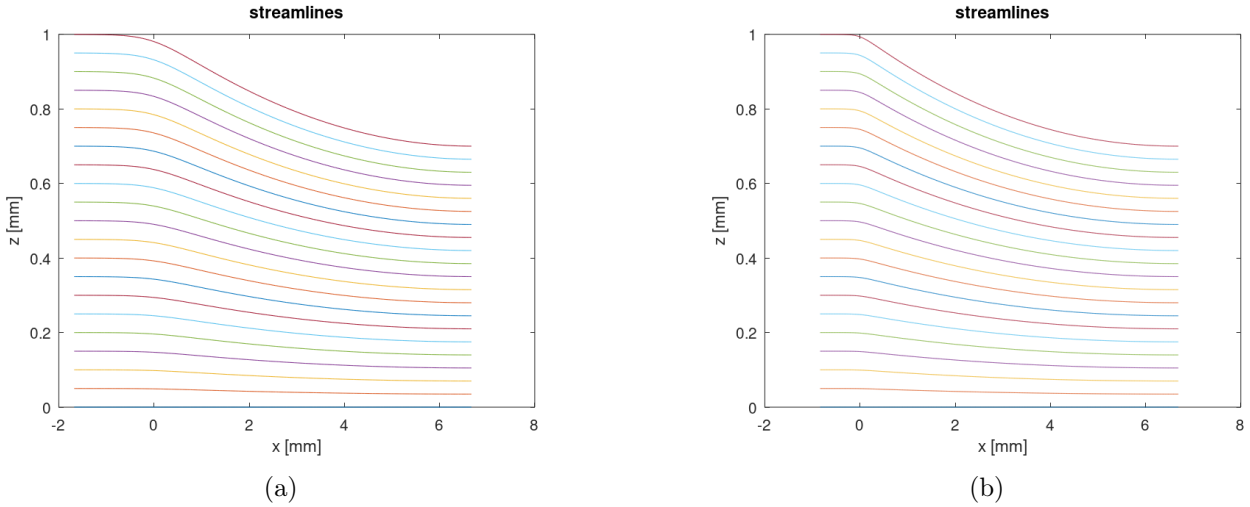

(a) (b)

Figure 8. Flowlines determined with the FLM (a) and mFLM (b) models

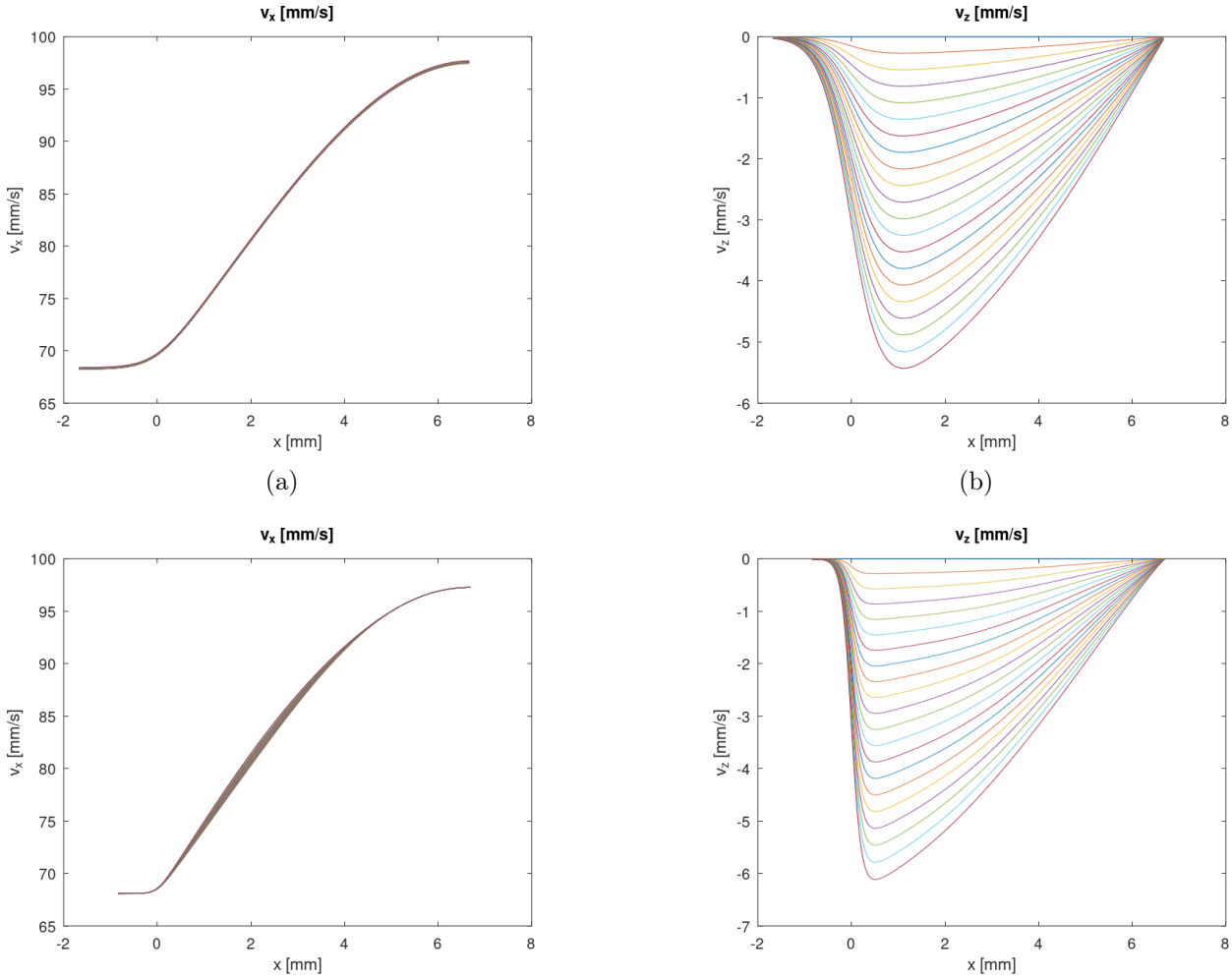

Figure 9. Velocity in x and z directions predicted by the FLM (a, b) and mFLM (c, d) models

of [1], where μ was estimated as 0.068. Based on the above analysis, one can conclude, that the friction coefficient can be derived from the FEM and mFLM simulations. The described FLM and

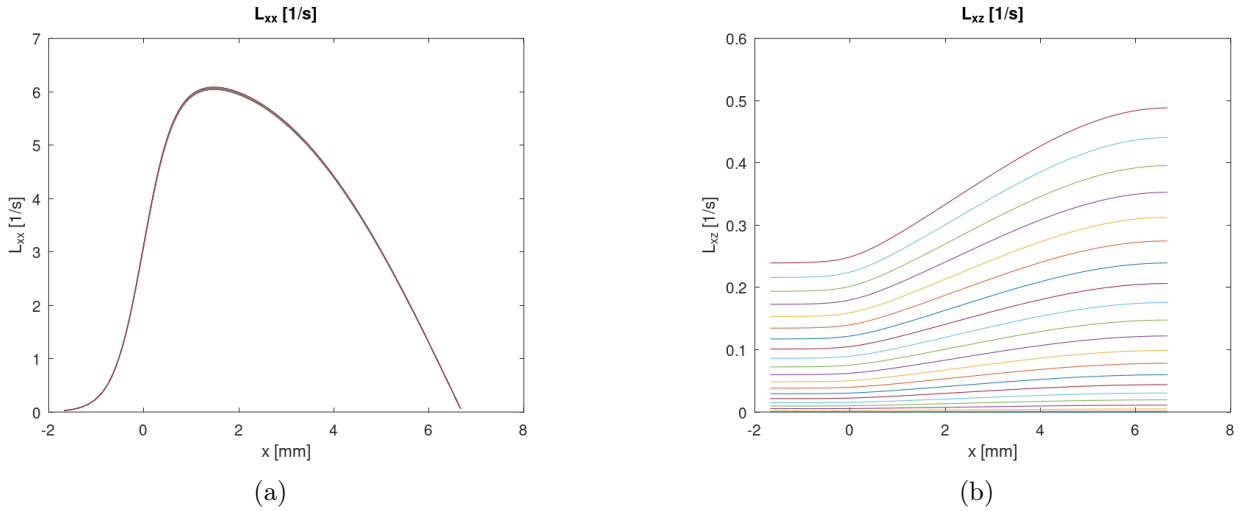

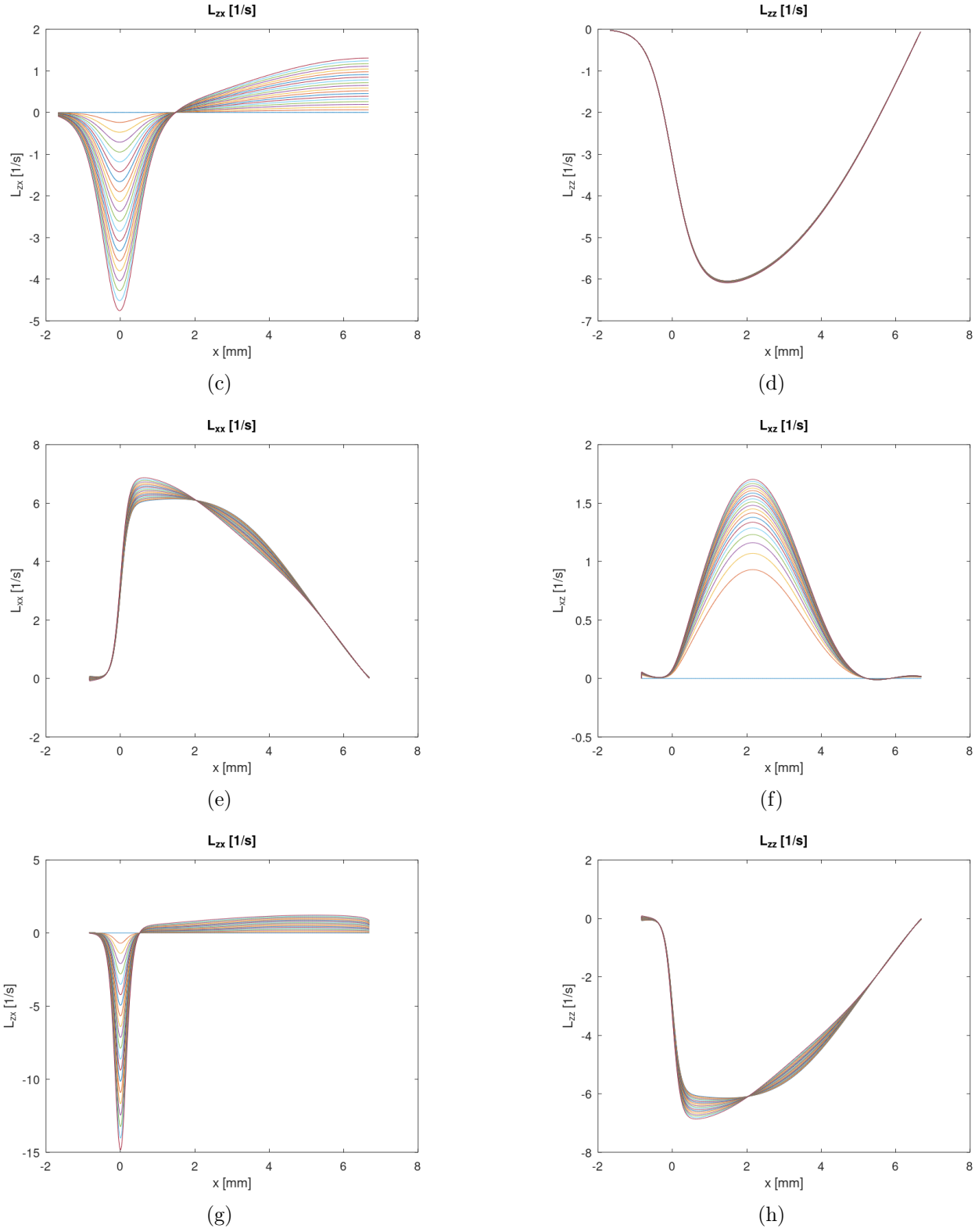

Figure 10. Velocity gradients in directions xx, xz, zx, and zz for FLM (a-d) and mFLM (e-h) models

mFLM models are solved by using GNU Octave numerical software package [41]. Comparison of the deformation flow as predicted by the FLM and mFLM are demonstrated in Figs. 9-11. Based only on the flowlines of Fig. 8(a) and 8(b), it can be concluded that there is a negligible difference between

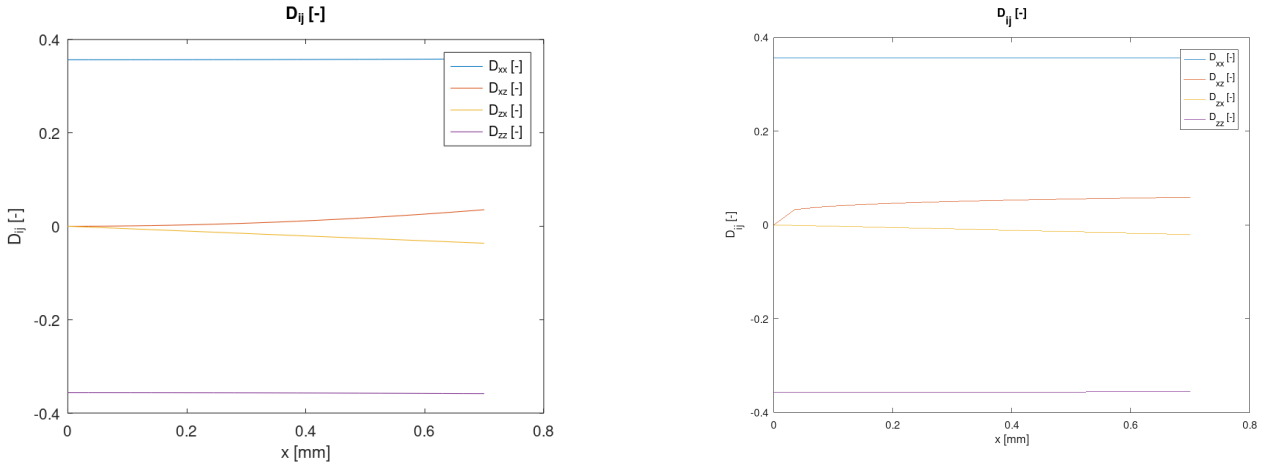

Figure 11. Strain components predicted by the FLM (a) and mFLM (b) models

the FLM and mFLM models. The difference is observed mainly near the entry part of the roll gap. Similar to the flowline models, differences in velocity are observable, especially in the direction z (Fig. 9(b), 9(d)).

It can be concluded, that directional velocity gradients are similar for FLM and mFLM only for xx (Fig. 10(b), 10(e)) and zz (Fig. 10(d), 10(h)) directions. In the case of the zx direction, the difference is higher compared to xx and zz directions. These deviations can be attributed to the different flowlines near to the entry point of the roll gap. For the direction xz, the difference between the two model predictions is quite noticeable, and the tendency of the lines is different between the FLM and mFLM models, however, the individual tendencies are corresponding to the models described in literature sources [24, 30] and [15, 31].

The calculated strain components in the rolled sheet by both FLM and mFLM models are shown in Fig. 11. As one can notice, the strain components are comparable to each other, while there is a slight difference near the mid-thickness of the rolled sheet. The shear strain values predicted by the models employed are given in Table 4. It seems that all methods tend to provide comparable shear strains.

8. Summary

In the present study, the measured deformation patterns of a rolled sheet are analyzed by various numerical approaches. The study suggests that the commonly used FEM model can be successfully employed for the simulation of the rolling process. The friction coefficient of 0.068 ensures a deformation flow in a cold rolled material with a 30% thickness reduction comparable to the experimentally observed one. Nearly identical value for the μ was predicted the Flow-Line Model employed [31].

Table 4. Shear strain values predicted by the models employed

Method	**Value**
Measured	$\gamma_s = 0.020$
FEM	$\gamma_s = 0.030$
FLM	$\gamma_s = 0.030$
mFLM	$\gamma_s = 0.025$

The minimum value of friction coefficient, necessary for cold rolling, as predicted by the analytical approach is comparable to ones derived by the FEM and FLM approaches. Both FEM and FLM methods were found to be suitable for describing the cold rolling, however, the computational time in case of FLM was orders of magnitude shorter as compared to FEM simulations.

In the later work, the model can be extended by the implementation of additional technological parameters, which will allow for: explaining the effect of heat generation, the nonuniformity of the friction coefficient, and the effect of the asymmetry due to different roll velocity. On the other hand, a new model can be developed for describing the anisotropy of the sheet's material, the hardening of the material, and its microstructural properties. In this way, a new, more precise material model will be used for the numerical simulations. The assessment of numerical approaches can be validated by relatively simple rolling trials.

9. Acknowledgement

Project no. TKP2021-NVA-29 has been implemented with the support provided by the Ministry of Innovation and Technology of Hungary from the National Research, Development and Innovation Fund, financed under the TKP2021-NVA funding scheme.

10. References

[1] J.Gy. Bátorfi, J.J. Sidor, *Alumínium lemez aszimmetrikus hengerlése közben fellépő deformációjának vizsgálata*, Mérnöki és Informatikai Megoldások|Engineering and IT Solutions, 2020. I, pp. 5–14, CrossRef

[2] B. Avitzur, *An upper-bound approach to cold-strip rolling*, Journal of Engineering for Industry 86(1), 1964, pp. 31–45, CrossRef

[3] M. Szűcs, Gy. Krallics, J.G. Lenard, *The difficulties of predicting the coefficient of friction in cold flat rolling*, Journal of Tribology 143(10), 2021, 101703, CrossRef

[4] A. Fischer, K. Bobzin, *Friction, wear and wear protection*, International Symposium on Friction, Wear and Wear Protection 2008, Aachen, Germany, Weinheim, Germany, Wiley-VCH, 2008.

[5] C. Cerbu, H. Teodorescu-Draghicescu, *Aspects on modeling the mechanical behavior of aluminum alloys with different heat treatments*, Journal of Computational and Applied Mechanics 12(2), 2017, pp. 85–98, CrossRef

[6] K. Santaoja, *Viscous and elastic-plastic material model in the ABAQUS*, Espoo: Technical Research Centre of Finland, 1993.

[7] G. Gadamchetty, A. Pandey, M. Gawture, *On Practical Implementation of the Ramberg-Osgood Model for FE Simulation*, SAE International Journal of Materials and Manufacturing 9(1), 2016, pp. 200–205, CrossRef

[8] W. Ramberg, W.R. Osgood, *Description of stress-strain curves by three parameters*, 1943, CrossRef

[9] O. Engler, J. Hirsch, *Texture control by thermomechanical processing of AA6xxx Al–Mg–Si sheet alloys for automotive applications — a review*, Materials Science and Engineering A 336(1–2), 2002, pp. 249–262, CrossRef

[10] C. Boldetti, C. Pinna, I.C. Howard, G. Gutierrez, *Measurement of deformation gradients in hot rolling of AA3004*, Experimental Mechanics 45(6), 2005, pp. 517–525, CrossRef

[11] R. Roumina, C.W. Sinclair, *Deformation geometry and through-thickness strain gradients in asymmetric rolling*, Metallurgical and Materials Transactions A 39(10), 2008, pp. 2495–2503, CrossRef

[12] C. Q. Ma, L.G. Hou, J.S. Zhang, L.Z. Zhuang, *Strain Analysis during the Symmetric and Asymmetric Rolling of 7075 Al Alloy Sheets*, In: M. Hyland (Ed.), Light Metals 2015, pp. 445–449, Springer International Publishing, CrossRef

[13] S.S. Dhinwal, L.S. Tóth, *Unlocking deformation path in asymmetric rolling by texture simulation*, Materials 13(1), 2019, 101, CrossRef

[14] M. Szűcs, Gy. Krállics, J. Lenard, *A comparative evaluation of predictive models of the flat rolling process*, Periodica Polytechnica Mechanical Engineering 62(2), 2018, pp. 165–172, CrossRef

[15] J.J. Sidor, *Assessment of flow-line model in rolling texture simulations*, Metals 9(10), 2019, 1098, CrossRef

[16] B. Avitzur, *Friction-aided strip rolling with unlimited reduction*, International Journal of Machine Tool Design and Research 20(3–4), 1980, pp. 197–210, CrossRef

[17] T. MiŁek, *The influence of friction coefficient on forward slip in experimental research on cold longitudinal flat rolling*, presented at the 10th Conference on Terotechnology, 2018, pp. 67-72, CrossRef

[18] Q.Y. Wang, Y. Zhu, Y. Zhao, *Friction and forward slip in high-speed cold rolling process of aluminum alloys*, Applied Mechanics and Materials 229–231, 2012, pp. 361–364, CrossRef

[19] H. Jin, D.J. Lloyd, The different effects of asymmetric rolling and surface friction on formation of shear texture in aluminium alloy AA5754, Materials Science and Technology 26(6), 2010, pp. 754–760, CrossRef

[20] M. Qwamizadeh, M. Kadkhodaei, M. Salimi, *Asymmetrical sheet rolling analysis and evaluation of developed curvature*, The International Journal of Advanced Manufacturing Technology 61(1–4), 2012, pp. 227–235, CrossRef

[21] G.-Y. Tzou, *Relationship between frictional coefficient and frictional factor in asymmetrical sheet rolling*, Journal of Materials Processing Technology 86(1–3), 1999, pp. 271–277, CrossRef

[22] L.A. de Carvalho, J. Ebrahim, Zs. Lukács, *The importance of pressure and velocity dependent friction coefficient in the metal forming simulation*, GÉP LXXII(1–2), 2021, pp. 11–14, CrossRef

[23] J.J. Sidor, P. Chakravarty, J.Gy. Bátorfi, P. Nagy, Q. Xie, J. Gubicza, *Assessment of dislocation density by various techniques in cold rolled 1050 aluminum alloy*, Metals 11(10), 2021, pp. 1571, CrossRef

[24] J.J. Sidor, R.H. Petrov, L. Kestens, *Texture control in aluminum sheets by conventional and asymmetric rolling*, In: Comprehensive Materials Processing, Elsevier, 2014, pp. 447–498, CrossRef

[25] J.Gy. Bátorfi, M. Andó, *Study of parameters during aluminum cutting with finite element method*, Periodica Polytechnica Mechanical Engineering 64(2), 2020, pp. 136–144, CrossRef

[26] J.Gy. Bátorfi, P. Chakravarty, J.J. Sidor, *Investigation of the wear of rolls in asymmetric rolling*, Mérnöki és Informatikai Megoldások|Engineering and IT Solutions 2021 II, pp. 14–20, CrossRef

[27] T. Inoue, *Strain variations on rolling condition in accumulative roll-bonding by finite element analysis*, In: D. Moratal (Ed.), Finite Element Analysis, Sciyo, 2010, CrossRef

[28] T. Inoue, H. Qiu, R. Ueji, *Through-thickness microstructure and strain distribution in steel sheets rolled in a large-diameter rolling process*, Metals 10(1), 2020, 91, CrossRef

[29] J. Fluhrer, *DEFORM(TM) 2D Version 8.1 User's Manual*, Scientific Forming Technolgies Corporation, CrossRef

[30] B. Beausir, L.S. Tóth, *A new flow function to model texture evolution in symmetric and asymmetric rolling*, In: A. Haldar, S. Suwas, D. Bhattacharjee (Eds.), Microstructure and Texture in Steels, London, Springer London, 2009, pp. 415–420, CrossRef

[31] K. Decroos, J.J. Sidor, M. Seefeldt, *A new analytical approach for the velocity field in rolling processes and its application in through-thickness texture prediction*, Metallurgical and Materials Transactions A 45(2), 2014, pp. 948–961, CrossRef

[32] F. Ďuroský, L. Zboray, Ž. Ferková, *Computation of rolling stand parameters by genetic algorithm*, Acta Polytechnica Hungarica 5(2), 2008, pp. 59–70.

[33] Y. Tian, Y. Guo, Z. Wang, G. Wang, *Analysis of rolling pressure in asymmetrical rolling process by slab method*, Journal of Iron and Steel Research International 16(4), 2009, pp. 22–26, CrossRef

[34] G. Hirt, S. Senge, *Selected processes and modeling techniques for rolled products*, Procedia Engineering 81, 2014, pp. 18–27, CrossRef

[35] Gy. Krállics, M. Szűcs, J. Lénárd, *Súrlódási tényező meghatározása lemez hideghengerlésnél*, Bányászati és Kohászati Lapok - Kohászat 145(2), 2012, pp. 3–6.

[36] A. Halloumi, Ch. Desrayaud, B. Bacroix, E. Rauch, F. Montheillet, *A simple analytical model of asymmetric rolling*, Archives of Metallurgy and Materials 57(2), 2012, pp. 425-435, CrossRef

[37] J.J. Minton, C.J. Cawthorn, E.J. Brambley, *Asymptotic analysis of asymmetric thin sheet rolling*, International Journal of Mechanical Sciences 113, 2016, pp. 36–48, CrossRef

[38] M. Mišović, N. Tadić, M. Jaćimović, M. Janjić, *Deformations and velocities during the cold rolling of aluminium alloys*, Materiali in tehnologije 50(1), 2016, pp. 59–67, CrossRef

[39] S.L. Oh, S. Kobayashi, *An approximate method for a three-dimensional analysis of rolling*, International Journal of Mechanical Sciences 17(4), 1975, pp. 293–305, CrossRef

[40] Y.-M. Hwang, T.-H. Chen, H.-H. Hsu, *Analysis of asymmetrical clad sheet rolling by stream function method*, International Journal of Mechanical Sciences 38(4), 1996, pp. 443–460, CrossRef

[41] J.W. Eaton, D. Bateman, S. Hauberg, *GNU Octave version 7.1.0 manual: a high-level interactive language for numerical computations*, 2022, CrossRef